Proceedings of the
47th IEEE Conference on Decision and Control
Cancun, Mexico, Dec. 9-11, 2008

A Passive 2DOF Walker: Finding Gait Cycles Using Virtual Holonomic Constraints

Leonid B. Freidovich, Uwe Mettin, Anton S. Shiriaev, Mark W. Spong.

Abstract— **A planar compass-like biped on a shallow slope is the simplest model of a passive walker. It is a two-degrees-of-freedom impulsive mechanical system known to possess periodic solutions reminiscent to human walking. Finding such solutions is a challenging task. We propose a new approach to obtain stable as well as unstable hybrid limit cycles without integrating the full set of differential equations. The procedure is based on exploring the idea of parameterizing a possible periodic solution via virtual holonomic constraints. We also show that a 2-dimensional manifold, defining the hybrid zero dynamics associated with a stable hybrid cycle, in general, is not invariant for the dynamics of the model of the compass-gait walker.**

Index Terms— **Walking Robots; Underactuated Mechanical Systems; Limit Cycles; Virtual Holonomic Constraints**

I. INTRODUCTION

The study of passive walking devices is a fascinating field. It attracted attention of researchers in the robotics and control communities after McGeer's publication in 1990 [11] presenting "*a class of two-legged machines for which walking is a natural dynamic mode*". It followed a series of publications, see e.g. [2]–[4], [7], [9], [10], [15], proposing and reporting various ways to find and to analyze passive gaits of walking devices. Successful results of passive walking are typically shown for quite simple models and it is not always clear how to generalize such findings to more realistic representations of walking robots with multiple degrees of freedom.

The main contribution of this paper is a new approach of searching for hybrid limit cycles of passive walking robots. We suggest analytical and constructive steps that allow to reduce, first, the number of parameters to be found in the search for suitable initial conditions, and second, the number of differential equations to be solved during the numerical procedure. Our demonstration is carried out for a standard benchmark example: the planar two-link walker commonly known as a compass-gait biped.

The key idea of the paper is exploring a special but generic change of coordinates that can always be used for parameterizing any nontrivial hybrid periodic solution of the walker dynamics. We avoid looking for explicit dependence on time but instead search for relations between the generalized coordinates that should be valid along a cycle. Such relations are called *virtual holonomic constraints* [13], [19]. Intuitively, the deviations from these geometric relations define a natural set of generalized coordinates in which a hybrid periodic motion has almost trivial representation, related to the canonical local coordinates introduced by Urabe [6], [18]. Results on using virtual holonomic constraints for motion planning and feedback controller design for mechanical systems can be found in [12], [13], [19] and others.

The analysis presented in the paper reveals important properties of hybrid periodic solutions of the walker dynamics. We show that the 2-dimensional manifold associated with a natural stable cycle, which is called hybrid zero dynamics in [20] and is broadly used for stabilization of walking gaits [19], in general, is not invariant for the hybrid dynamics of a compass-gait walker. This observation, made for a natural cycle of a passive mechanical system, is important for analysis, synthesis, and stabilization of 'natural gaits' for controlled walking robots. Currently, the concept of hybrid zero dynamics and methods for its stabilization are well developed [19] following the pioneering works of [5], [20] and are becoming of common use. The observed here lack of such invariance for a natural gait of a passive walker motivates development of other approaches.

II. HYBRID DYNAMICS OF THE COMPASS-GAIT BIPED

Let us consider a two-link passive compass-gait biped robot, schematically shown on Fig. 1.

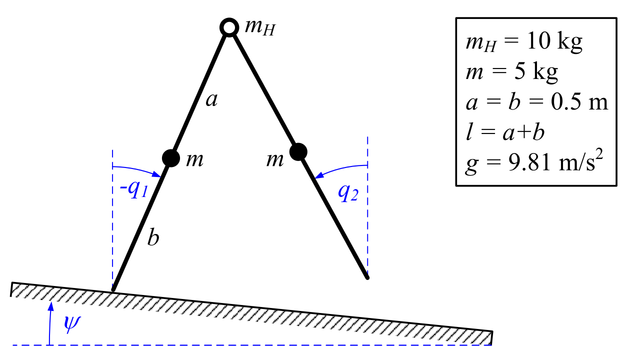

Fig. 1. Schematic of the compass-gait biped on a shallow slope ψ.

Under certain conditions [4], the dynamics of the robot can be described [4], [7], [16] by the following system of Euler–

L. Freidovich and U. Mettin are with the Department of Applied Physics and Electronics, Umeå University, SE-901 87 Umeå, Sweden. E-mail: {Leonid.Freidovich|Uwe.Mettin}@tfe.umu.se.

A. Shiriaev is with the Department of Applied Physics and Electronics, Umeå University, SE-901 87 Umeå, and the Department of Engineering Cybernetics, Norwegian University of Science and Technology, NO-7491 Trondheim, Norway. E-mail: Anton.Shiriaev@tfe.umu.se.

M. Spong is with the Coordinated Science Laboratory, University of Illinois at Urbana-Champaign, Urbana, IL 61801, USA. E-mail: mspong@uiuc.edu

This work has been partly supported by the Kempe Foundation, the Swedish Research Council (under grant 2005-4182), and by the U.S. National Science Foundation (under grant CMMI-0510119).

Lagrange equations with impulsive effects [1], [5], [19]

$$\begin{aligned} &\frac{d}{dt}\left[\frac{\partial \mathcal{L}(q,\dot q)}{\partial \dot q}\right] - \frac{\partial \mathcal{L}(q,\dot q)}{\partial q} = 0 && \text{for} \quad q \notin \mathcal{S} \\ &q^+ = P\,q^- \quad \text{and} \quad \dot q^+ = P_q(q^-)\,\dot q^- && q^- \in \mathcal{S} \end{aligned} \tag{1}$$

where $q = [q_1,\, q_2]^T$ is the vector of generalized coordinates. The Lagrangian is given by

$$\mathcal{L}(q,\dot q) = \frac{1}{2}\,\dot q^T M(q)\,\dot q - V(q)$$

with the positive definite matrix of inertia

$$M(q) = \left[\begin{array}{cc} p_1 & -p_2\cos(q_1-q_2) \\ -p_2\cos(q_1-q_2) & p_3 \end{array}\right]$$

and the potential energy

$$V(q) = p_4\,(\cos(q_1) - 1) + p_5\,(1 - \cos(q_2))\,.$$

Here the coefficients of the Largangian are defined by the physical parameters of the robot (listed in Fig. 1) as follows

$$\begin{aligned} &p_1 = (m_H + m)l^2 + ma^2, \quad p_2 = mlb, \quad p_3 = mb^2, \\ &p_4 = (m_H l + ma + ml)g, \quad p_5 = mbg \end{aligned}$$

Given the slope ψ of the walking surface, the impact surface is defined by

$$\mathcal{S} = \left\{q \in \mathbb{R}^2: \quad H(q) = \cos(q_1+\psi) - \cos(q_2+\psi) = 0\right\} \tag{2}$$

The impulse-effects are described by the renaming matrix

$$P = \left[\begin{array}{cc} 0 & 1 \\ 1 & 0 \end{array}\right] \tag{3}$$

and the reset map

$$P_q(q^-) = \left[\begin{array}{cc} p_{11}^+ & p_{12}^+ \\ p_{21}^+ & p_{22}^+ \end{array}\right]^{-1} \left[\begin{array}{cc} p_{11}^- & p_{12}^- \\ p_{21}^- & p_{22}^- \end{array}\right] \tag{4}$$

with $p_6 = m \cdot a \cdot b,\ p_7 = (m_H \cdot l^2 + 2m \cdot a \cdot l)$,

$$\begin{aligned} p_{11}^+ &= p_1 - p_2\,\cos(q_1^- - q_2^-) \\ p_{12}^+ &= p_3 - p_2\,\cos(q_1^- - q_2^-) \\ p_{21}^+ &= -p_2\,\cos(q_1^- - q_2^-), \qquad p_{22}^+ = p_3 \\ p_{11}^- &= -p_6 + p_7\,\cos(q_1^- - q_2^-) \\ p_{12}^- &= -p_6, \qquad p_{21}^- = -p_6, \qquad p_{22}^- = 0 \end{aligned}$$

that attributes the jump in velocities due to impact [5], [8], [16]; here the notations

$$q^- = \lim_{\tau\to t-} q(\tau) \qquad \text{and} \qquad q^+ = \lim_{\tau\to t+} q(\tau)$$

are used for the states right before and right after the impact.

As known, the equations (1) can be rewritten as (see [17])

$$M(q)\,\ddot q + C(q,\dot q)\,\dot q + G(q) = 0 \tag{5}$$

with corresponding matrix functions $C(\cdot)$ and $G(\cdot)$.

Our goal is to find symmetric walking gaits[1] of the hybrid mechanical system (1).

[1]Arguments used for finding a symmetric gait are generic and can be therefore similarly applied to asymmetric gaits.

III. Procedure of Finding Hybrid Limit Cycles Using Virtual Holonomic Constraints

A. Notation for the parameters of a cycle

Given a shallow slope ψ, a symmetric periodic solution of (1) is uniquely defined by the vector of parameters[2]

$$p_\star = \left[\begin{array}{ccccccccc} a, & b, & c, & d, & e, & f, & g, & h, & T \end{array}\right]^T \in \mathbb{R}^9$$

consisting of the half-period $T = T_p/2 > 0$ and the following 8 constants, denoting the initial and final states,

$$\begin{aligned} q_\star(0+) &= \left[q_{1\star}(0+),\, q_{2\star}(0+)\right]^T = \left[a,\, e\right]^T \\ \dot q_\star(0+) &= \left[\dot q_{1\star}(0+),\, \dot q_{2\star}(0+)\right]^T = \left[b,\, f\right]^T \\ q_\star(T-) &= \left[q_{1\star}(T-),\, q_{2\star}(T-)\right]^T = \left[c,\, g\right]^T \\ \dot q_\star(T-) &= \left[\dot q_{1\star}(T-),\, \dot q_{2\star}(T-)\right]^T = \left[d,\, h\right]^T \end{aligned} \tag{6}$$

B. Relations among the parameters of a cycle

After each step the robot experiences an impact if it hits the ground, i.e. the condition (2) is satisfied. It follows from $q_\star(T_-) \in \mathcal{S}$ that

$$\cos(c+\psi) - \cos(g+\psi) = 0 \tag{7}$$

Note that the swing leg of a rigid two-link walker trespasses the impact surface (2) during one complete step. Following the other researchers, for our considerations, we assume that the compass-gait robot experiences an impact only when a heel strike occurs.

The impulse effect (instantaneous change of the states), described by the second equation in (1) together with (3) and (4), gives the following expressions for the reset states after impact

$$\begin{aligned} &\left[\begin{array}{c} a \\ e \end{array}\right] = P\left[\begin{array}{c} c \\ g \end{array}\right] = \left[\begin{array}{c} g \\ c \end{array}\right] \qquad \text{and} \\ &\left[\begin{array}{c} b \\ f \end{array}\right] = P_q\!\left(\left[\begin{array}{c} c \\ g \end{array}\right]\right)\left[\begin{array}{c} d \\ h \end{array}\right] \end{aligned} \tag{8}$$

Solving the system of five algebraic equations (7) and (8) in terms of a, b, d, one obtains

$$\begin{aligned} g &= a\,, \quad c = e = -a - 2\,\psi \\ f &= \frac{b\cos\left(2\,a + 2\,\psi\right)p_2 - p_6 d}{p_3} \\ h &= \frac{d(p_3p_7 - p_6p_2) - b(p_3p_1 - p_2^2\cos 2(a+\psi))}{p_3p_6}\cos 2(a+\psi) \end{aligned} \tag{9}$$

Solving[3] the continuous-time dynamics (5), i.e. 4 first-order differential equations, on the time interval $0 \le t \le T$ one can obtain 4 missing relations for defining the parameters a, b, d, and T of the cycle. So that the search of a hybrid cycle

[2]The parameters a and b here are not related to the notation for the physical lengths given in Fig. 1.

[3]numerically or symbolically

is converted into the search of the minimizer (the vector of parameter p_*) for the optimization problem:

$$\left.\begin{array}{l} \min\limits_{\{a,b,d,T\}} \left\{ \left\| \bar q(T) - \begin{bmatrix} c \\ g \end{bmatrix} \right\|^2 + \left\| \dot{\bar q}(T) - \begin{bmatrix} d \\ h \end{bmatrix} \right\|^2 : \right. \\ \quad \text{with (9) satisfied and } \bar q(t) \text{ being} \\ \quad \text{the solution of (5) initiated at} \\ \quad \bar q(0) = \begin{bmatrix} a \\ e \end{bmatrix}, \quad \dot{\bar q}(0) = \begin{bmatrix} b \\ f \end{bmatrix} \end{array} \right\} \tag{10}$$

The optimization problem (10) is standard, and typically solved through numerical integration of the system dynamics (5). Such approach largely depends on a chosen integration method, and might be of limited use for detecting a stable cycle with small region of attraction and for detecting unstable periodic motions. Let us develop an alternative procedure.

C. Hunting for cycles using virtual holonomic constraints

The continuous sub-arc of a nontrivial periodic trajectory $q_\star(t)$ for (1), if exists, is a solution of the differential equations (5) defined on a finite interval of time. Hence, the evolution of the generalized coordinates along the cycle can be specified not only as periodic functions of time

$$q_\star(t) = q_\star(t+T_p) = [q_{1\star}(t),\, q_{2\star}(t)]^T, \qquad \forall\, t$$

but also as functions of a scalar variable that uniquely defines a particular point on the continuous sub-arc of the cycle

$$\begin{array}{l} q_{1\star}(t) = \phi_1(\theta_\star(t)), \quad q_{2\star}(t) = \phi_2(\theta_\star(t)) \\ \text{for} \quad 0 < t < T = T_p/2 \end{array}$$

The shape of functions $\phi_1(\cdot)$, $\phi_2(\cdot)$ depends on the way we parameterize points on the trajectory of the cycle in the state space of the walker, but these functions are clearly unique for each parametrization.

If we assume that the new variable $\theta_\star$ is one of the generalized coordinates, let say the coordinate of stance leg, then the re-parameterization results in a new representation

$$q_{1\star}(t) = \theta_\star(t),\; q_{2\star}(t) = \phi(\theta_\star(t)), \text{ for } 0 < t < T \tag{11}$$

of continuous sub-arc of the cycle between two consecutive impacts. The scalar functions $\theta_\star(\cdot)$ and $\phi(\cdot)$ are unknown. To derive equations with respect to these variables, we can use the dynamics of the robot, i.e. substitute the relations[4]

$$q_1 = \theta, \qquad q_2 = \varphi(\theta) \tag{12}$$

into the Euler–Lagrange equations (5) and collect some terms. The straightforward computations result into two differential equations of the 2^{nd} order for the θ-variable

$$\alpha_1(\theta)\, \tfrac{d^2}{dt^2}\theta + \beta_1(\theta)\, \left[\tfrac{d}{dt}\theta\right]^2 + \gamma_1(\theta) \;=\; 0 \tag{13}$$

$$\alpha_2(\theta)\, \tfrac{d^2}{dt^2}\theta + \beta_2(\theta)\, \left[\tfrac{d}{dt}\theta\right]^2 + \gamma_2(\theta) \;=\; 0 \tag{14}$$

where $\gamma_1(\theta) = -p_4 \sin(\theta)$, $\gamma_2(\theta) = p_5 \sin(\varphi(\theta))$ and

$$\begin{array}{l} \alpha_1(\theta) = -p_2 \cos(\theta - \varphi(\theta))\, \varphi'(\theta) + p_1 \\ \beta_1(\theta) = -p_2 \sin(\theta - \varphi(\theta))(\varphi'(\theta))^2 - p_2 \cos(\theta - \varphi(\theta))\varphi''(\theta) \\ \alpha_2(\theta) = -p_2 \cos(\theta - \varphi(\theta)) + p_3\, \varphi'(\theta) \\ \beta_2(\theta) = p_2 \sin(\theta - \varphi(\theta)) + p_3\, \varphi''(\theta) \end{array}$$

[4]Such relations between generalized coordinates of the system are known as virtual holonomic constraint, see e.g. [12], [19].

At first glance, the equations (13), (14) are similar to the Euler–Lagrange equations (5). Indeed, the relations (12) can be seen as a change of generalized coordinates for the system. Meanwhile, each of the second-order nonlinear differential equations (13), (14) with respect to time, can be rewritten as a first-order linear differential equation with θ as an independent variable:

$$\tfrac{1}{2}\alpha_1(\theta)\, \tfrac{d}{d\theta}\left(\left[\tfrac{d}{dt}\theta\right]^2\right) + \beta_1(\theta)\, \left[\tfrac{d}{dt}\theta\right]^2 + \gamma_1(\theta) = 0 \tag{15}$$

$$\tfrac{1}{2}\alpha_2(\theta)\, \tfrac{d}{d\theta}\left(\left[\tfrac{d}{dt}\theta\right]^2\right) + \beta_2(\theta)\, \left[\tfrac{d}{dt}\theta\right]^2 + \gamma_2(\theta) = 0 \tag{16}$$

and can be integrated [14] independent on the from of the functions $\alpha_i(\cdot)$, $\beta_i(\cdot)$, and $\gamma_i(\cdot)$, $i = 1,\, 2$.

Lemma 1 (Integral and energy): *Along any solution $\theta(t)$ of the nonlinear system*

$$\alpha(\theta)\, \ddot\theta + \beta(\theta)\, \dot\theta^2 + \gamma(\theta) = 0 \tag{17}$$

(a) *the integral function*

$$I\Big(\theta, \dot\theta, \theta(0), \dot\theta(0)\Big) = \dot\theta^2 - e^{\left\{-\int\limits_{\theta(0)}^{\theta} \frac{2\beta(\tau)}{\alpha(\tau)}\, d\tau\right\}} \dot\theta^2(0) + \int_{\theta(0)}^{\theta} e^{\left\{\int\limits_{\theta}^{s} \frac{2\beta(\tau)}{\alpha(\tau)}\, d\tau\right\}} \frac{2\gamma(s)}{\alpha(s)} ds \tag{18}$$

preserves its zero value

$$I\Big(\theta(t), \dot\theta(t), \theta(0), \dot\theta(0)\Big) \equiv 0$$

for all $t \geq 0$ for which the solution $\theta(t)$ is defined;

(b) *the energy function, if defined for some constant x,*

$$E_x(\theta, \dot\theta) = \frac{1}{2} \underbrace{e^{\left\{\int\limits_{x}^{\theta} \frac{2\beta(\tau)}{\alpha(\tau)} d\tau\right\}}}_{\Psi_x(\theta)} \dot\theta^2 + \int\limits_{x}^{\theta} \frac{\gamma(\tau)}{\alpha(\tau)} \Psi_x(\tau) d\tau \tag{19}$$

preserves its value $E_x\Big(\theta(t), \dot\theta(t)\Big) \equiv E_x\Big(\theta(0), \dot\theta(0)\Big)$. In particular

$$E_x\Big(\theta(0+), \dot\theta(0+)\Big) \equiv E_x\Big(\theta(T-), \dot\theta(T-)\Big)$$

for the the time moments right after an impact and right before the next impact. ■

The identities in (a) and (b) can be checked via direct computations. Proof for (a) can be found in [14]. The identity in (b) means simply that there is no change in the energy-like function (19) for any solutions of (17) between impacts.

Both equations (13), (14) are in the form (17); therefore, they have two conserved quantities (18) or two energies (19) irrespective of the particular form of the unknown function $\phi(\cdot)$. Having in mind that dynamics of the walker is not completely integrable, presence of two conserved quantities for (13), (14) is indeed surprising. The explanation for this apparent contradiction is that the conserved quantities are not true first integrals of the system and are solution dependent.

It is worth to observe that not only the equations (13), (14) are of the form (17), but any linear combination of the equations (13), (14) with θ-dependent weights $\mu_1(\theta)$, $\mu_2(\theta)$ has again the form of (17) with the coefficients

$$\begin{bmatrix} \alpha(\theta) \\ \beta(\theta) \\ \gamma(\theta) \end{bmatrix} = \begin{bmatrix} \alpha_1(\theta) & \alpha_2(\theta) \\ \beta_1(\theta) & \beta_2(\theta) \\ \gamma_1(\theta) & \gamma_2(\theta) \end{bmatrix} \begin{bmatrix} \mu_1(\theta) \\ \mu_2(\theta) \end{bmatrix}$$

For instance, with the weights

$$\mu_1(\theta) = 1, \quad \mu_2(\theta) = \varphi'(\theta)$$

one restores the true energy of the Euler–Lagrange system

$$E(q, \dot q) = \frac{1}{2}\, \dot q^T\, M(q)\, \dot q + V(q)$$

when the generalized coordinates are not any but satisfy the relations (12), i.e.

$$\begin{aligned} & E(q,\dot q)|_{\{q_1=\theta,\, q_2=\varphi(\theta),\, \dot q_1=\dot\theta,\, \dot q_2=\varphi'(\theta)\dot\theta\}} = E_0(\theta,\dot\theta) \\ & = \left(\tfrac{p_1}{2} - p_2\, \cos(\theta-\varphi(\theta))\varphi'(\theta) + \tfrac{p_3}{2}(\varphi'(\theta))^2\right)\dot\theta^2 \\ & \quad +p_4\left[\cos(\theta)-1\right] + p_5\left[1-\cos(\varphi(\theta))\right] \end{aligned} \tag{20}$$

Here the function $E_0(\cdot)$ is $E_x(\cdot)$ from (19) with $x = 0$.

If the velocities before and after each impact are non-zero[5], so that $b \neq 0$ and $d \neq 0$, then the boundary conditions (6) can be rewritten in terms of the virtual holonomic constraint (11) as follows

$$\begin{array}{llll} \theta_\star(0) = a, & \dot\theta_\star(0) = b, & \theta_\star(T) = c, & \dot\theta_\star(T) = d \\ \varphi(a) = e, & \varphi'(a) = \frac{f}{b}, & \varphi(c) = g, & \varphi'(c) = \frac{h}{d} \end{array} \tag{21}$$

As $E_x(\cdot)$ keeps its value, see Lemma 1, one can substitute the relations (21) into the function (20) obtain another identity between the parameters of the cycle defined in (6)

$$\begin{aligned} E_0(c,d) = E_0(a,b) \overset{(9)}{=} & \tfrac{p_1\, b^2}{2} - p_2\, \cos(a-e)\, f\, b \\ & + \tfrac{p_3\, f^2}{2} + p_4(\cos(a)-1) + p_5(1-\cos(e)) \end{aligned} \tag{22}$$

As seen, it is a quadratic equation with respect to d, so at best it has two real solutions for given values of a and b.

Reducing the number of parameters to search for in (10) is not the only benefit of using virtual constraints. Let us now reduce the number of differential equations needed to be solved during the search: One can look at the system of differential equations (13) and (14) as a system of algebraic equations for the two unknown functions of time $\dot\theta_\star^2(t)$ and $\ddot\theta_\star(t)$. To derive a differential equation for the function $\varphi(\cdot)$ used for re-parameterization of evolution of generalized coordinates $q_\star(t)$ along the cycle, consider two cases:

- **Case 1: The function** $D(\theta) := \big(\beta_1(\theta)\alpha_2(\theta) - \beta_2(\theta)\alpha_1(\theta)\big)$ **is separated from zero on a sub-arc of the cycle, i.e.** $D(\theta_\star(t)) \neq 0$ **for** $0 \le t_0 \le t \le t_1 \le T$**.**[6] For this time interval $[t_0, t_1]$ the differential equations (13) and (14) can be solved as algebraic ones w.r.t. $\dot\theta_\star^2(t)$ and $\ddot\theta_\star(t)$ as follows

$$\dot\theta_\star^2 = \frac{\alpha_2(\theta_\star)\gamma_1(\theta_\star) - \alpha_1(\theta_\star)\gamma_2(\theta_\star)}{\alpha_1(\theta_\star)\beta_2(\theta_\star) - \alpha_2(\theta_\star)\beta_1(\theta_\star)} \tag{23}$$

$$\ddot\theta_\star = \frac{\beta_1(\theta_\star)\gamma_2(\theta_\star) - \beta_2(\theta_\star)\gamma_1(\theta_\star)}{\alpha_1(\theta_\star)\beta_2(\theta_\star) - \alpha_2(\theta_\star)\beta_1(\theta_\star)} \tag{24}$$

The equation (23) in conjunction with the relation on the energy (22) rewritten as

$$\dot\theta^2 = \frac{E_0(a,b) - p_4(\cos(\theta)-1) - p_5(1-\cos(\varphi(\theta)))}{\frac{p_1}{2} - p_2\, \cos(\theta-\varphi(\theta))\, \varphi'(\theta) + \frac{p_3}{2}\, (\varphi'(\theta))^2} \tag{25}$$

results in the 2^{nd} order equation for the function $\varphi(\cdot)$

$$\varphi''(\theta_\star) = f_1\left(a, b, \theta_\star, \varphi(\theta_\star), \varphi'(\theta_\star)\right) \tag{26}$$

where the right-hand side is found by symbolic computation.

- **Case 2: The function** $D(\theta) := \big(\beta_1(\theta)\alpha_2(\theta) - \beta_2(\theta)\alpha_1(\theta)\big)$ **is zero on a sub-arc of the cycle, i.e.** $D(\theta_\star(t)) \equiv 0$ **for** $0 \le t_0 \le t \le t_1 \le T$**.** For this time interval the identity $D(\theta_\star(t)) \equiv 0$ can be used and rewritten as differential equation for φ. Manipulating on (13) and (14) gives another identity which combined with the previous yields the following first order equation

$$\varphi'(\theta_\star) = f_2\left(\theta_\star, \varphi(\theta_\star)\right) \tag{27}$$

where the right-hand side is found by symbolic computation.

The arguments above are summarized as a new procedure to find limit cycles for symmetric gaits of the passive compass-gait biped:

Proposition 1 (Procedure to find limit cycles): *A symmetric walking gait of the passive compass-like robot (1) on a shallow slope ψ is defined in terms of 8 parameters (6) representing initial and final states right after and right before impact.*

(a) *The renaming matrix (3) and the reset map (4) that apply to the states when impact occurs yield 5 algebraic equations (9) for the parameters g, c, e, f, and h expressed in terms of the values of a, b, and d.*

(b) *Introducing the virtual holonomic constraint (11) allows to reparameterize a particular trajectory of (1) that corresponds to continuous-time dynamics between impacts by a solution of (17). The initial and final states (6) are then given by (21).*

(c) *Lemma 1 gives an expression for the conserved energy (22) between impacts, which yields two solutions for the parameter d that can be written as functions of a and b.*

(d) *Finally, only two parameters a and b are left as variables; they are to be found numerically as minimizers, for which the following performance index attains zero value:*

$$\begin{aligned} \min_{\{a,b\}} \Big\{ & \ |\bar\varphi(c) - g|^2 + |\bar\varphi'(c) - h/d|^2 : \\ & \text{with (9) and (22) satisfied} \\ & \text{and } \bar\varphi(\theta) \text{ satisfies either (26) or (27)} \\ & \text{initiated at } \bar\varphi(a) = e \text{ and } \bar\varphi'(a) = f/b \Big\} \end{aligned} \tag{28}$$

(e) *As soon as the limit cycle is found, its period can be computed using the following formula*

$$T = \int_c^a \sqrt{\frac{\frac{p_1}{2} - p_2 \cos(\theta-\varphi_\star(\theta))\varphi_\star'(\theta) + \frac{p_3}{2}(\varphi_\star'(\theta))^2}{E_0(a,b) - p_4(\cos(\theta)-1) - p_5(1-\cos(\varphi_\star(\theta)))}}\, d\theta$$

Here $\varphi_\star(\theta)$ is the constraint function for the periodic motion.

Clearly, (28) is simpler than (10). The fact that the conserved quantity (20) depends on the function $\varphi(\theta)$ and its two derivatives point-wise, and not in a functional way through integration, allows to reduce by one both the number of parameters and the order of the system of the differential equations to solve. The other reduction is due to searching for a solution in the form without explicit dependence on time.

IV. RESULTS: SYMMETRIC GAIT CYCLES OBTAINED FROM ANALYSIS

Here we elaborate the arguments of the previous section and organize the search for symmetric gaits of the passive walker with parameters listed in Fig. 1. The shallow slope for the compass-gait

[5]This is a natural assumption.

[6]Note that the condition $D(\theta_\star(t)) \neq 0$ was always satisfied in our numerical studies.

biped is chosen in a range of $\psi \in (0, 6]\,\mathrm{deg}$ which is about the same interval as discussed in [4]. The initial conditions $q_\star(0+)$ and $\dot q_\star(0+)$, as well as the half-period T and the total energy E_0 of the found symmetric gaits for this range of the slope angle are shown in Fig. 2 and Fig. 3 as functions of ψ. As seen, two

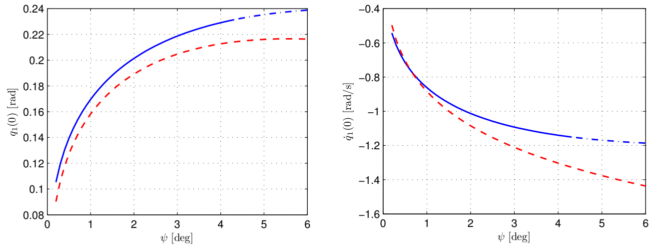

(a) Initial position $q_{\star,1}(0+)$ for the stance leg.

(b) Initial velocity $\dot q_{\star,1}(0+)$ for the stance leg.

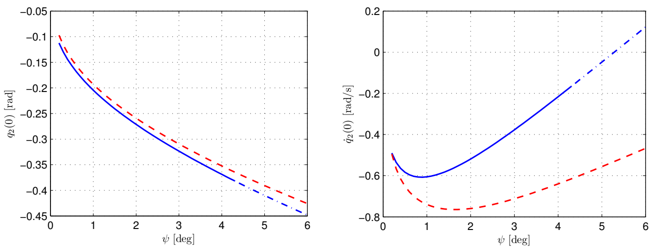

(c) Initial position $q_{\star,2}(0+)$ for the swing leg.

(d) Initial velocity $\dot q_{\star,2}(0+)$ for the swing leg.

Fig. 2. Initial conditions for the two symmetric gait cycles obtained from analysis (*solid line* corresponds to stable cycles).

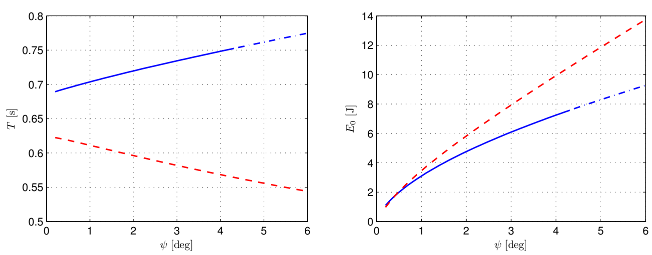

(a) Resulting half-period T.

(b) Required total energy E_0.

Fig. 3. Half-period and total energy of the two symmetric gait cycles obtained from analysis (*solid line* corresponds to stable cycles).

hybrid limit cycles are found following the proposed arguments. It turns out that these cycles can be distinguished by two different solutions for d, which we expected according to Proposition 1(c). One limit cycle (represented by the dashed line in Fig. 2) is always unstable. The other limit cycle (represented by the solid line in Fig. 2) is exponentially orbitally stable within the interval $\psi \in (0, \sim 4.4)\,\mathrm{deg}$ and unstable otherwise. For slopes $\psi \geq\sim 4.4\,\mathrm{deg}$ one can then notice a change in the stability properties caused by bifurcation which makes the symmetric gait cycle unstable, but results in asymmetric gait cycles for the robot.

V. Is Zero Dynamics Invariant for a Hybrid Walking Gait?

For a stable walking cycle of the passive compass-gait walker, it is of interest to explore properties of the system dynamics and especially to make some insights into mechanism of its orbital stability. Re-parametrization of this cycle by one of generalized coordinates, i.e. through a virtual holonomic constraint, as done above, might be a good staring point. Indeed, the recently proposed concept of *hybrid zero dynamics* and associated control architectures [19], [20] are explicitly based on this re-parametrization. They are among a few control design methods that achieve orbital stabilization of walking gaits. So, it is of interest to understand to what extend the concept of *hybrid zero dynamics* is appropriate and relevant for naturally stable walking cycles.

To this end, consider the stable gait cycle (Fig 4a) with $\psi = 2.87\,[\mathrm{deg}]$ and

$$\begin{array}{rcl} q_\star(0+) & \approx & \big[0.21689,\ -0.31708\big]^T\ [\mathrm{rad}] \\ \dot q_\star(0+) & \approx & \big[-1.08428,\ -0.39728\big]^T\ [\mathrm{rad/s}] \end{array} \qquad (29)$$

The *virtual holonomic constraints* corresponding to this cycle are

$$q_{\star,1}(t) = \theta_\star(t), \quad q_{\star,2}(t) = \varphi_\star(\theta_\star(t)), \qquad (30)$$

where the function $\varphi_\star(\theta_\star(t))$ depicted on Fig 4b, is the solution of the system (26) with (units omitted)

$$\begin{array}{l} a = 0.21689, \quad b = -1.08428, \quad \theta_\star(0) = 0.21689 \\ \varphi(\theta_\star(0)) = -0.31708, \quad \varphi'(\theta_\star(0)) = 0.36640 \end{array}$$

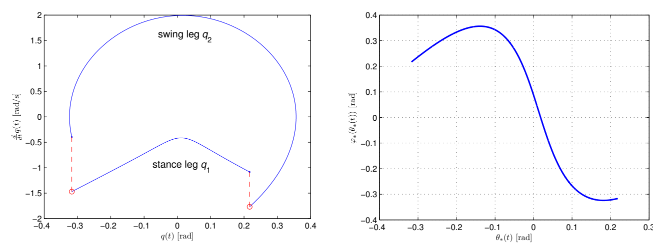

(a) Phase portrait.

(b) Virtual holonomic constraint.

Fig. 4. Symmetric gait cycle (29).

The hybrid zero dynamics $\mathcal{Z}$ associated with the functions (30) is defined as a subset of the state space of the walker dynamics

$$\mathcal{Z} = \Big\{[q_1, q_2, \dot q_1, \dot q_2] : q_2 = \varphi_\star(q_1), \dot q_2 = \Big[\tfrac{d}{dq_1}\varphi_\star(q_1)\Big]\dot q_1\Big\} \qquad (31)$$

and in the vicinity of the cycle it is a 2-dimensional smooth sub-manifold of the state space. Intersections of $\mathcal{Z}$ with impact surface $\mathcal{S}$, see (2), will define two curves γ_+ and γ_-. Then, invariance of *hybrid zero dynamics* consists of two conditions:

1) Invariance of $\mathcal{Z}$ with respect to the vector field of continuous-in-time part of the walker dynamics: if initial conditions belong to a non-trivial subset of $\gamma_+ \subset \mathcal{Z}\bigcap\mathcal{S}$, then the solution of the Euler–Lagrange equations (1) obey to stay on $\mathcal{Z}$ until the next impact occurs; ending up on $\gamma_- \subset \mathcal{Z}\bigcap\mathcal{S}$.
2) Invariance of $\mathcal{Z}$ with respect to the impact: an appropriate non-trivial subset of the curve γ_- is mapped by the impact update law of (1) into an appropriate non-trivial subset of the curve γ_+.

Below we consider both conditions for invariance separately, starting with the second one.

A. Invariance of hybrid zero dynamics on the switching surfaces

Lemma 2: For any non-trivial symmetric gait of the compass gait walker (1) the associated hybrid zero dynamics is invariant with respect to the update law due to an impact. ■

The proof is omitted due to limitations of space. However, the arguments are generic and can be applied for non-symmetric gaits, as well as can be readily extended for gaits of higher-dimensional planar bipeds. It follows that the corresponding requirements on the choice of the constraint functions in [19], [20] are natural.

B. Lack of invariance of hybrid zero dynamics for the continuous-in-time vector field

Invariance of the zero manifold $\mathcal{Z}$ for the vector field of the two-link walker can be tested through some theoretical arguments, or through computer simulation elaborated for some cycles. At the moment, we cannot bring affirmative reasoning proving that such invariance is hardly possible. Meanwhile, all numerical simulations strongly support the conclusion: *hybrid zero dynamics is not invariant for the continuous-in-time vector field of the walker dynamics*.

On Figs. 5 the motions of the two-link walker initialized at points on the curve γ_+ other than $[q_\star(t),\, \dot q_\star(t)]$, are shown together with the target cycle (29), (30). As seen, the solutions do not end up on the curve γ_- upon the intersecting switching surface Γ_-.

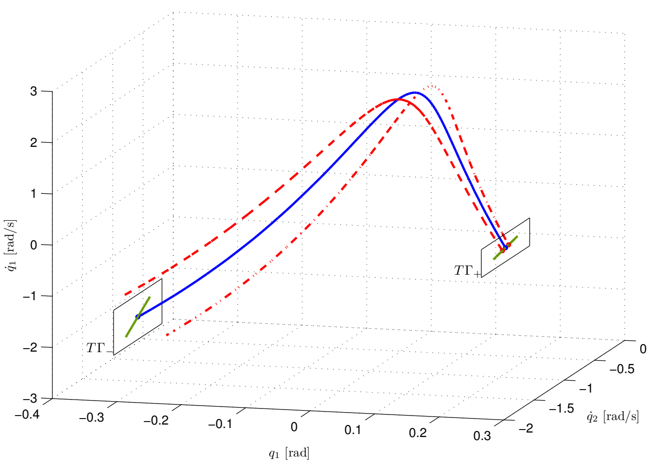

Fig. 5. Desired trajectory (*solid*) in the subspace $\{q_1,\, \dot q_1,\, \dot q_2\}$ with continuous-time sub-arc evolving between the hypersurfaces Γ_+ and Γ_-. The discrete mapping is invariant, i.e. $F(\gamma_-) \subset \gamma_+$. However, trajectories starting on γ_+ other than $[q_\star(t),\, \dot q_\star(t)]$ do not end up in γ_- (see *dashed* and *dashed-dotted* trajectories), i.e. the zero dynamics, defined by the trajectory of the cycle, are not invariant.

VI. Conclusion

The problem of finding hybrid periodic trajectories for a model of compass-gait biped robot, consisting of a 2 DOF Euler–Lagrange dynamics and an instantaneous impact map is studied. Straightforward computations lead to a minimization problem, which requires finding four parameters and is based on solving a 4^{th}-order differential equation for computation of the target functional.

Noticing that there must be a geometric relation between the two generalized coordinates along the continuous-time sub-arc of any periodic trajectory, we have obtained dynamics projected onto a manifold defined by the corresponding virtual holonomic constraint. We have discovered that such dynamics can be described by two independent integrable differential equations. As a result, one can obtain a third-order differential equation for the function describing the constraint and furthermore reduce it to a second-order differential equation exploiting the analytical expression for one of the conserved quantities. Our computations lead to a minimization problem, which requires finding two parameters and is based on solving the found second-order differential equation for computation of the target functional. So, the burden of numerical computations is reduced in half.

We have verified that the proposed computational procedure does work and allows finding stable as well as unstable limit cycles for a reasonable range of the slopes of the walking surface.

We have also studied applicability of the concept of hybrid zero dynamics. It has been shown that, in general, the corresponding two-dimensional manifold induced by the periodic trajectory is not invariant. It is of interest to notice that the discovered absence of invariance is in the continuous part of the dynamics while in the discrete part invariance is always naturally present.

We believe that our approach is generalizable to a description of a passive walking biped in the form of a system of Euler–Lagrange equations of arbitrary order with an instantaneous updating law modeling impact with the walking surface. However, it is left for future investigations.

References

[1] D. Bainov and P. Simeonov, *Systems with Impulse Effects: Stability, Theory and Applications*, ser. Ellis Horwood Series: Mathematics and its Applications. Chichester: Ellis Horwood, 1989.

[2] S. Collins, A. Ruina, R. Tedrake, and M. Wisse, "Efficient bipedal robots based on passive dynamic walkers," *Science Magazine*, vol. 307, pp. 1082–1085, 2005.

[3] A. Goswami, B. Espiau, and A. Keramane, "Limit cycles in a passive compass gait biped and passivity-mimicking control laws," *Journal of Autonomous Robots*, vol. 4, no. 3, pp. 273–286, 1997.

[4] A. Goswami, B. Thuilot, and B. Espiau, "A study of the passive gait of a compass-like biped robot," *International Journal of Robotics Research*, vol. 17, no. 12, pp. 1282–1301, 1998.

[5] J. Grizzle, G. Abba, and F. Plestan, "Asymptotically stable walking for biped robots: Analysis via systems with impulse effects," *IEEE Transactions on Automatic Control*, vol. 46, no. 1, pp. 51–64, 2001.

[6] J. Hale, *Ordinary Differential Equations*. Malabar: Krieger, 1980.

[7] I. Hiskens, "Stability of hybrid system limit cycles: Application to the compass gait biped robot," in *Proceedings of the 40th IEEE Conference on Decision and Control*, Orlando, USA, Dec. 4-7, 2001.

[8] Y. Hurmuzlu and D. Marghitu, "Rigid body collisions of planar kinematic chains with multiple contact points," *International Journal of Robotics Research*, vol. 13, no. 1, pp. 82–92, 1994.

[9] A. Kuo, "Stabilization of lateral motion in passive dynamic walking," *International Journal of Robotics Research*, vol. 18, no. 9, pp. 917–930, 1999.

[10] ——, "Choosing your steps carefully: Trade-offs between economy and versatility in dynamic walking bipedal robots," *IEEE Robotics and Automation Magazine*, vol. 14, no. 2, pp. 18–29, 2007.

[11] T. McGeer, "Passive dynamic walking," *International Journal of Robotics Research*, vol. 9, no. 2, pp. 62–82, 1990.

[12] A. Shiriaev, L. Freidovich, and I. Manchester, "Can we make a robot ballerina perform a pirouette? Orbital stabilization of periodic motions of underactuated mechanical systems," *Annual Reviews in Control*, 2008.

[13] A. Shiriaev, J. Perram, and C. Canudas-de-Wit, "Constructive tool for orbital stabilization of underactuated nonlinear systems: Virtual constraints approach," *IEEE Transactions on Automatic Control*, vol. 50, no. 8, pp. 1164–1176, 2005.

[14] A. Shiriaev, J. Perram, A. Robertsson, and A. Sandberg, "Periodic motion planning for virtually constrained Euler–Lagrange systems," *Systems and Control Letters*, vol. 55, pp. 900–907, 2006.

[15] M. Spong and F. Bullo, "Controlled symmetries and passive walking," *IEEE Transactions on Automatic Control*, vol. 50, no. 7, pp. 1025–1031, 2005.

[16] M. Spong, J. Holm, and D. Lee, "Passivity-based control of bipedal locomotion," *IEEE Robotics and Automation Magazine*, vol. 14, no. 2, pp. 30–40, 2007.

[17] M. Spong, S. Hutchinson, and M. Vidyasagar, *Robot Modeling and Control*. Hoboken, New Jersey: John Wiley and Sons, 2006.

[18] M. Urabe, *Nonlinear Autonomous Oscillations*. New York: Academic Press, 1967.

[19] E. Westervelt, J. Grizzle, C. Chevallereau, J. Choi, and B. Morris, *Feedback Control of Dynamic Bipedal Robot Locomotion*. CRC Press, Taylor and Francis Group, 2007.

[20] E. Westervelt, J. Grizzle, and D. Koditschek, "Hybrid zero dynamics of planar biped walkers," *IEEE Transactions on Automatic Control*, vol. 48, no. 1, pp. 42–56, 2003.